CHEMISTRY OF MATERIALS

Article

pubs.acs.org/cm

Fabrication of Binary and Ternary Hybrid Particles Based on Colloidal Lithography

Ye Yu,[†] Bin Ai,[†] Helmuth Möhwald,[‡] Ziwei Zhou,[†] Gang Zhang,*[,†] and Bai Yang[†]

[†]State Key Lab of Supramolecular Structure and Materials, College of Chemistry, Jilin University, Changchun 130012, People's Republic of China

[‡]Max Planck Institute of Colloids and Interfaces, D-14424 Potsdam, Germany

Supporting Information

ABSTRACT: We describe a versatile strategy for engineering binary and ternary hybrid particles (HPs) through a combination of etching and deposition processes based on colloidal lithography (CL). Non-close-packed (ncp) polymer colloidal crystals were used as both original seed microparticles and templates for generating hybrid patches. Utilizing chemical or plasmonic etching procedures, the hybrid patches were generated underneath the colloidal template and were successfully attached on the microspheres through thermal treatment. The hybrid particles composing metals and polymers were tunable in size, composition, and morphology. This method provides a versatile and modular tool to fabricate similar hybrid microparticles and/or nanoparticles that, integrated into predesigned materials, promise applications in photonic and magnetic devices.

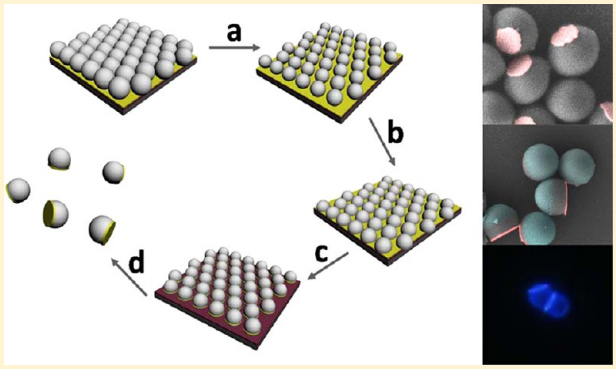

KEYWORDS: *hybrid particle, asymmetric, binary, ternary, colloidal lithography, heterogeneous*

1. INTRODUCTION

Increased attention has been given to the fabrication and application of colloidal particles with asymmetric shape and structure, as well as tunable composition; such particles are known as asymmetric colloidal particles. Progress in nanotechnology has made it possible to construct numerous asymmetric colloidal particles with different functionalities. Special methods have been developed to fabricate asymmetric colloidal particle surfaces, such as toposelective surface modification,[1−4] template-directed self-assembly,[5] controlled phase separation,[6,7] surface nucleation,[8−10] and microfluidic strategies.[11] Because of their unique properties, these asymmetric colloidal particles have potential applications such as use in self-propelling micromachines,[12] as building blocks for "bottom-up" or self-assembly approaches to micropatterns,[13−16] and for the fabrication of optical and magnetic devices.[17−19]

Hybrid colloidal particles, as a class of asymmetric colloidal particles, are an extension from single-component particles to hybrid structures with discrete domains of different materials, and they have also attracted considerable attention, because they may possess unique and integrative properties that cannot be obtained via one single component. Granick and co-workers reported methods to fabricate "triblock" colloids by functionalization of colloidal microspheres with three or more zones of chemical functionality, and these triblock colloids could be directly self-assembled into various complex lattice structures.[20] Sacanna et al. introduced a new class of spherical colloids with microscopic permanent magnets embedded underneath the surface of colloids, which could reversibly self-assemble into well-defined nonlinear structures.[21] By now, many methods have been used to generate hybrid colloidal particles, and each of them possesses unique advantages and limitations. In all of these methods, colloidal lithography (CL) was widely used to fabricate complex structures and colloidal particles of varying size, shape, and morphology. In general, CL uses two-dimensional (2D) or three-dimensional (3D) colloidal crystals as masks,[22−25] templates,[26−29] or objects[30−32] for depositing or etching. This unconventional technique of lithography leads to various sorts of unique patterning scalable down to submicrometer and nanometer scale both on plane and curved surfaces. Although some impressive efforts have been made in their fabrication and application, there is still a strong need to develop a versatile approach to complex structures on hybrid colloidal particles.

In this paper, we introduce a versatile method to fabricate hybrid colloidal particles with designed size, shape, and morphology. With the aid of colloidal lithography and controlled diverse etching processes, we successfully generated several types of binary/ternary hybrid particles (HPs), as demonstrated for combinations of gold, nickel, silver, copper, poly(methylmethacrylate) (PMMA), and polystyrene (PS).

Received: August 3, 2012
Revised: November 5, 2012
Published: November 6, 2012

Scheme 1. Schematic Sketch Detailing the Different Options for the Fabrication of Hybrid Particles: (I) O_2 Plasma Etching, (II) Slight Thermal Treatment, (III) Adequate Thermal Treatment, (IV) Reactive Ion Etching, (V) Wet Chemical Etching, (VI) Releasing from the Substrate, (VII) O_2 Plasma Etching, (VIII) second deposition, and (IX) Original Substrate Left Behind

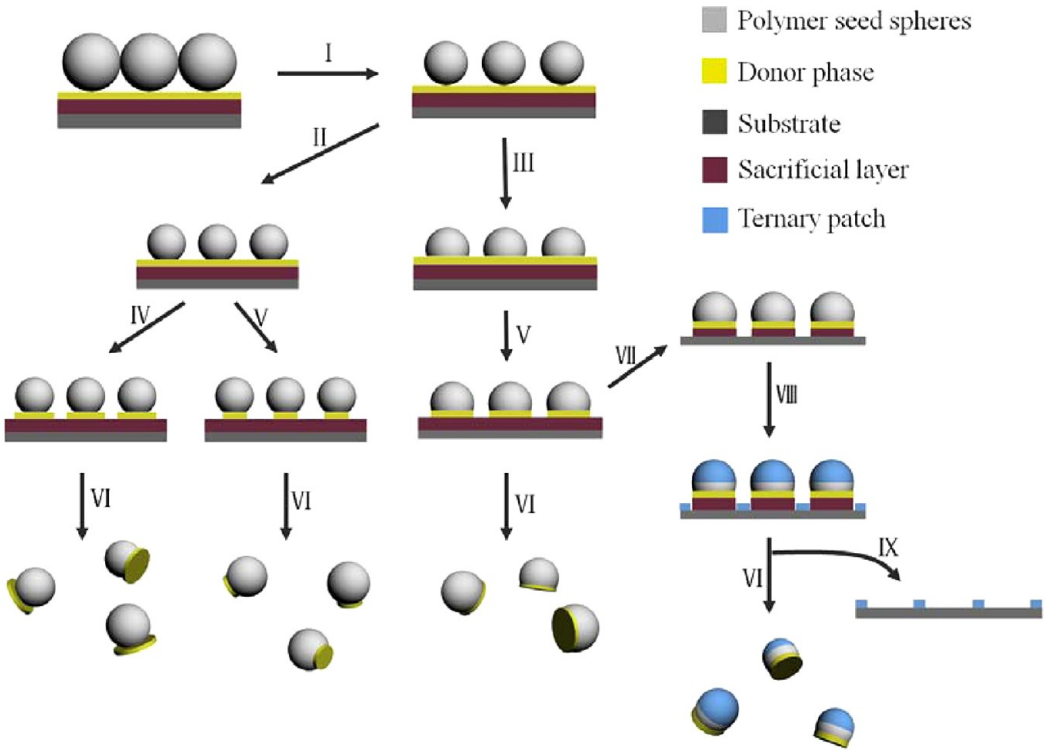

This way of fabrication of HPs could easily be expanded to any other combination of materials that can be etched. The resulting HPs not only retain their individual magnetic and luminescent properties but these properties are also present simultaneously.

2. EXPERIMENTAL SECTION

Chemicals and Materials. Polystyrene (PS) spheres in diameters of 210 and 580 nm were prepared by emulsion polymerization, as described in ref 33. PS spheres (1 μm) were purchased from Sigma–Aldrich, and 3-μm PS spheres were obtained from Wuhan Tech Co., Ltd. 1-Methoxy-2-propanol-acetate (MPA) and poly(methylmethacrylate) (PMMA) (M_w = 120 000) were purchased from Aldrich. 4-(Diphenylamino) benzaldehyde (4-DPAB) was purchased from Fluka. Silicon(100) wafers were cleaned by immersion into a solution of concentrated H_2SO_4:H_2O_2 (v/v: 7/3) for ~5 h at 90 °C and then rinsed repeatedly with Milli-Q water (18.2 MΩ cm) and ethanol, then finally dried by a stream of nitrogen gas. *[Caution: This concentrated H_2SO_4:H_2O_2 solution is a strong oxide!]* Amorphous silicon bulk (99.99%) was purchased from KYKY Technology Development Co., Ltd. Au (99.999%), and Ni (99.99%) were purchased from Sinopharm Chemical Reagent Co., Ltd. Photoresist (BP212-37 positive photoresist, Kempur (Beijing) Microelectronics, Inc.) was used as received or diluted with MPA. Gold etchant (KI/I_2 based) was purchased from Transene Company, Inc., and diluted with deionized water before use. Sodium dodecylsulfate (SDS), sulfuric acid, hydrogen peroxide, hydrofluoric acid, potassium hydroxide, toluene, and ethanol were purchased from Beijing Chemical Works, and were used as-received.*[Caution: Hydrofluoric acid is highly toxic!]*

Preparation of the Donor Phase. Herein, gold, silicon, and 4-DPAB@PMMA were chosen as the donor phases that were attached to the PS microspheres. Films of photoresin with different thicknesses were first spin-coated onto the Si wafer and cured for 2–4 h at 130 °C as sacrificial layers for easier dispersion. After that, gold or silicon was deposited onto the as-prepared substrate. A 4-DPAB@PMMA film was spin-coated onto the glass substrate at 3000 rpm for 1 min. (Details are shown in section 1.1 in the Supporting Information.)

Preparation of Non-Close-Packed 2D PS Colloidal Crystals. The PS microsphere monolayers were prepared by the interface method.[34] To prepare the non-close-packed (ncp) 2D colloidal crystals, oxygen plasma was produced by a modified plasma cleaner. For PS colloidal crystals (3 μm) on 4-DPAB@PMMA, oxygen reactive ion etching (RIE) operating at a pressure of 35 mTorr, a flow rate of 50 sccm, and a radio-frequency (RF) power of 100 W, an inductively coupled plasma (ICP) power of 300 W was applied for 1–6 min on a Plasmalab Oxford 80 Plus system. The shape and size of the ncp PS colloidal crystals were modified by thermal treatment at 110–115 °C for 10–15 min. (Details also on the interface method to prepare a colloidal crystal are shown in section 1.2 in the Supporting Information.)

Preparation of Binary Hybrid Particles. After the ncp PS colloidal crystals were fabricated via oxygen plasma and thermal treatment, the exposed donor phase was etched away. For the 30-nm gold donor phase, the as-prepared samples were immersed in the gold etchant for 10–12 s, followed by rinsing with copious amounts of DI water. (Details are shown in section 1.3 in the Supporting Information.)

Preparation of Ternary Hybrid Particles. The upper hemispheres of the as-prepared binary HPs were further modified utilizing physical vapor deposition. After the binary HPs were fabricated according to the description above, nickel metal vapor was deposited on the as-prepared samples to obtain a thickness of 10 or 20 nm. The metal vapor was deposited perpendicularly onto the sample, and ternary HPs were thus generated. (Details are given in section 1.4 in the Supporting Information.)

Preparation of Free-Standing Hybrid Particles. The HPs were released by soaking into corrosive solution to etch away the substrate, and were washed by centrifugation at a speed of 6000–8000 rpm for 10 min and sonication for 3–5 times. (Details are given in section 1.5 in the Supporting Information.)

dx.doi.org/10.1021/cm3024692 | *Chem. Mater.* 2012, 24, 4549–4555

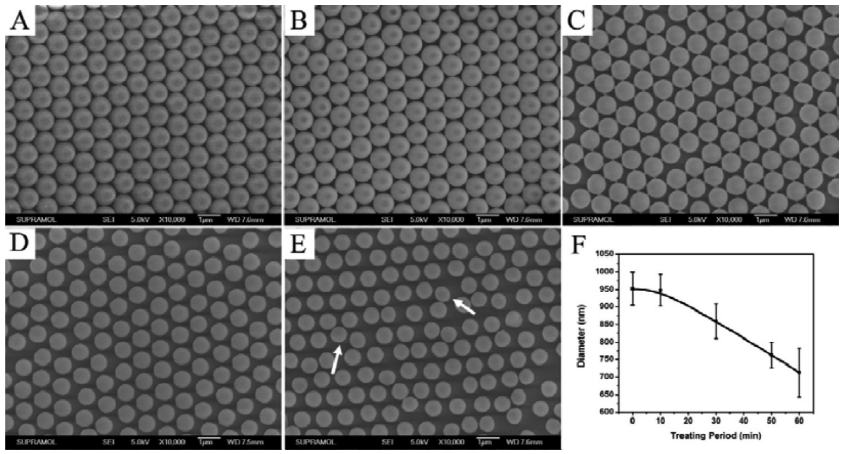

Figure 1. SEM images of PS colloidal crystals under oxygen plasma treatment. The oxygen plasma etching duration was (A) 0 min, (B) 10 min, (C) 30 min, (D) 50 min, and (E) 60 min. Panel (F) shows the development of diameters of PS with etching duration. The white arrows point to the PS spheres that were disturbed from the original situation during the O_2 treatment.

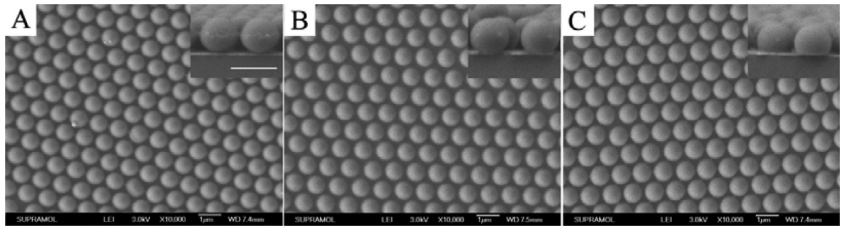

Figure 2. SEM images of ncp PS colloidal crystal (A) before thermal treatment and (B, C) after thermal treatment. The heating conditions were 110 °C for 10 min (B) and 110 °C for 15 min (C). The scale bar in the inset image is 1 μm.

Characterization. SEM micrographs were taken with a JEOL Model FESEM 6700F electron microscope with a primary electron energy of 3 kV. An energy-dispersive X-ray spectroscopy (EDS) detector coupled with an SEM system (Model XL 30 ESEM FEG scanning electron microscope, FEI Company) was used for elemental analysis. To get better images, the samples with asymmetric nanoparticles and nanoshells were sputter-coated with 2 nm of platinum before imaging. Fluorescence photo images were taken with an Olympus fluorescence microscope (Model BX51). TEM was conducted using a Hitachi Model H-800 electron microscope at an acceleration voltage of 200 kV with a CCD camera.

3. RESULTS AND DISCUSSION

Binary and ternary hybrid particles were generated through colloidal lithography combining deposition and etching processes. As shown in Scheme 1, the donor phase was first deposited or spin-coated on a glass slide or a sacrificial layer. A single-layered hexagonal-close-packed (hcp) PS colloidal crystal then was transferred to the as-prepared substrate via the interface method. Through O_2 plasma treatment, the hcp PS colloidal crystal was turned into a ncp one, leaving sufficient interspace for further thermal treatment. By appropriate thermal treatment, the binding ability between PS seed particles and the donor phase beneath was enhanced. After the exposed donor phase was etched away, binary HPs were generated. The ternary HPs were fabricated by vapor deposition on the as-prepared binary HPs. The hybrid particles then were released from the substrate by dissolving the sacrificial layer, followed by washing for several times. The detailed options of binary and ternary HPs were also shown, which includes several typical HPs fabricated through adjusting the types of donor phase, thermal treatment, and proper etching processes.

3.1. Formation of ncp PS Sphere Arrays.

Here, we took PS-Au hybrid particles as an example for binary spherical HPs. On the substrate, first, a film of photoresist as a sacrificial layer was spin-coated, and then Au was deposited as a donor phase. Before deposition, the sacrificial layer was cured for 2−4 h at a temperature of 130 °C, which makes it stable in deposition and also easy to remove. After that, the single-layered hcp PS colloidal crystal (1 μm) was transferred to the as-prepared substrate via the interface method.[34]

Oxygen plasma treatment was utilized for 10 min repeatedly to generate a ncp PS colloidal crystal with varied lattice spacing. As shown in Figure 1, the hcp PS colloidal crystal was treated for 0 min (Figure 1A), 10 min (Figure 1B), 30 min (Figure 1C), 50 min (Figure 1D), and 60 min (Figure 1E). The diameters of PS colloidal spheres can be continuously reduced by increasing the etching duration. Furthermore, when the etching duration was below 30 min, the adjacent PS colloidal spheres were connected with small dots, while, after continuing etching for 40 and 50 min, the connecting small dots disappeared. When the etching duration was further increased to 60 min, the ncp colloidal PS spheres showed slightly random orientation, indicated by the white arrows in Figure 1E. The disturbance may be caused by the long time treatment because of the low power of the plasma cleaner. The diameter of PS decreases with etching time from 952 nm (Figure 1A) to 713 nm (Figure 1E), and this is quantified in Figure 1F. Finally, we took 50 min as the proper oxygen plasma treatment condition, where the diameter of PS spheres was 763 nm. Because after 50 min of etching, the colloidal PS spheres were successfully detached from each other, sufficient interspace for further thermal treatment was left, but, at the same time, the highly ordered colloidal crystals were well-maintained.

dx.doi.org/10.1021/cm3024692 | *Chem. Mater.* 2012, 24, 4549−4555

The ncp PS colloidal crystals with controlled interspace thus fabricated were then heated to 110 °C for 10 and 15 min, respectively. Through tuning the heating temperature and period, the shape and attachment area with the donor phase could be controlled (Scheme 1, steps II and III). Figure 2 showed the ncp PS colloidal crystal before (Figure 2A) and after (Figures 2B and 2C) thermal treatment. The as-prepared ncp PS colloidal spheres were evidently mushroom-shaped instead of spherical-shaped (Figure 2A, inset image). After heating, the mushroom-like PS became globular and no connection was found between adjacent PS colloidal spheres. The area attached to the donor phase was increased when the heating duration was prolonged (insets of Figures 2B and 2C). The heating process was not only the key for controlling the size of the donor phase, but also afforded sufficient flexibility in combining PS spheres and donor phase (gold). The PS-Au HPs were more stable after adequate heating.

3.2. Preparation of Binary Hybrid Particles. After controlled heating, the PS spheres reshaped to original spherical morphology and were attached to the donor phase with a certain area beneath. The attached area acted as a mask while fabricating binary HPs. The bare donor phase at the interspace of the PS spheres could be etched away to generate individual HPs. Here, we chose gold to be the donor phase, as an example. The 30-nm uncovered gold donor phase was chemically etched away with a gold etchant for 10−12 s. Because of the hydrophobicity of the samples (PS spheres and gold films are both hydrophobic materials), the gold etchant was difficult to wet, which hindered the chemical etching process. To overcome the poor wettability, the samples were treated by O_2 plasma for 10 s to increase the hydrophilicity before chemical etching.

As shown in Figure 3A, the PS sphere mask was peeled off with tape after chemical etching of gold, leaving the individual donor disks on the substrate. The gold donor disks were well-defined and uniform in size and shape. The binary HPs then were released from the substrate by dissolving the sacrificial layer with KOH aqueous solution (1 M). After several times of centrifugation and sonication with water and ethanol, the binary HPs were deposited on the Si wafer for SEM imaging (Figure 3B). The shape of the PS spheres could easily be tuned by oxygen reactive ion etching (RIE). In Figure 3C, the PS spheres were treated by oblique oxygen RIE to form the nonspherical HPs. The incidence angle of the reactive oxygen ion beam was 60°. The colloidal PS spheres were anisotropic in shape after oblique oxygen RIE. From the top view and side view of the PS colloidal arrays (Figure 3C), it is revealed that the anisotropic PS seeds were highly oriented. The oxygen RIE could not disrupt the colloidal crystal, and the change in morphology was distinct from that without treatment. The binary nonspherical PS-Au HPs were released and washed as described above. In Figure 3D, the anisotropy of the PS part was well-displayed. EDS mapping of the PS-Au HPs (see Figure S1 in the Supporting Information) also showed the well-defined distribution of PS seed spheres and the gold donor disks. The as-prepared HPs were stable during the process of dissolution of the sacrificial layer and drying on a surface for imaging. Mild sonication and centrifugation did not destroy the binary HPs. Most of the gold donor disks adhered to the colloidal PS spheres, and the average yield of the PS-Au binary HPs was 85% (over 2000 particles were counted).

In our fabrication method, the heating process is a crucial step, because it determines the size of the donor phase attached on the PS colloidal spheres. Basically, we chose two thermal conditions: 110 °C for 10 min (Figure 4A) and 15 min (Figure 4B). During the heating process, the size of the attaching-donor-phase area was increased by prolonging the heating duration, as shown in Figure 2. Thus, binary PS-Au HPs with small or large gold donor disks were fabricated, respectively. Through controlling the thermal conditions, HPs with defined size of the donor phase were thus successfully fabricated.

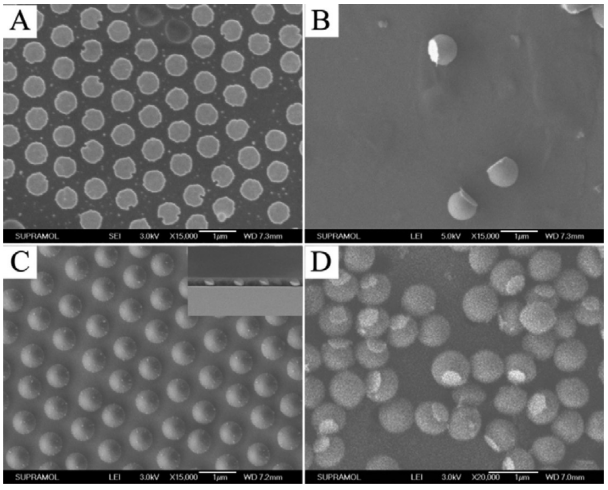

Figure 3. SEM images of binary spherical HPs and nonspherical HPs: (A) the individual gold donor disk arrays on the sacrificial layer, (B) released PS-Au binary spherical HPs, (C) nonspherical PS colloidal crystal after oblique oxygen RIE treatment, and (D) released PS-Au binary nonspherical HPs.

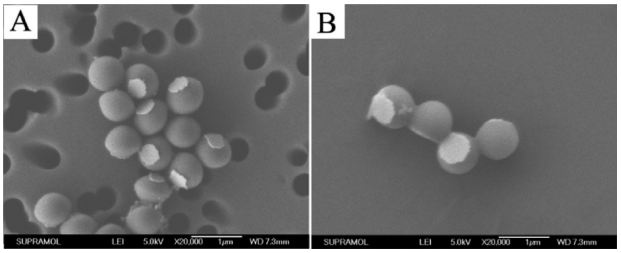

Figure 4. SEM images of binary PS-Au HPs with (A) small and (B) large gold donor disks. The heating conditions were 110 °C for 10 (panel A) and 15 min (panel B), respectively.

One advantage of the CL technique is to easily adjust the feature size simply by changing the diameters of the colloidal spheres. In Figure 5, we have fabricated binary PS-Au HPs with different diameters. The original diameters of the PS colloidal spheres were 1 μm (Figures 5A and 5B), 580 nm (Figures 5C and 5D), and 210 nm (Figures 5E and 5F). Using SEM and TEM, the morphology of the HPs was clearly revealed. Binary PS-Au HPs as small as 200 nm were generated, indicating that HPs could be fabricated through our method, even in ranges from 200 nm to 1 μm. Figure 5F shows that the diameter of the gold donor disks was ~40−50 nm, indicating that the highest resolution of wet chemical etching have reached 160 nm. It is generally most difficult to fabricate nanostructures a few hundred nanometers in size by chemical etching; thus, we are especially satisfied that binary PS-Au HPs <200 nm in diameter could be obtained.

dx.doi.org/10.1021/cm3024692 | *Chem. Mater.* 2012, 24, 4549−4555

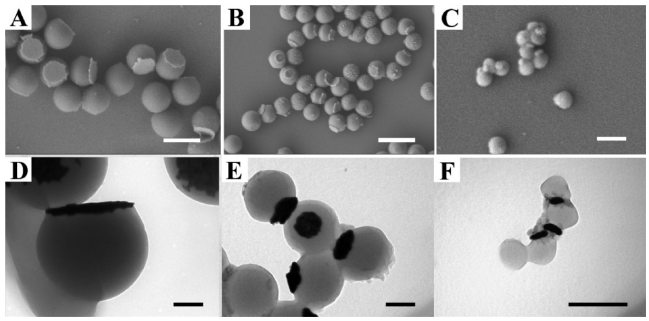

Figure 5. (A, B, C) SEM and (D, E, F) TEM images of binary PS-Au HPs with different diameters. The scale bars are 1 μm in panels (A) and (B), and 200 nm in panels (C), (D), (E), and (F). The original diameters of the PS spheres were 1 μm (A, D), 580 nm (B, E), and 210 nm (C, F).

Besides PS-Au HPs, polymeric HPs were also fabricated through a similar procedure. Instead of chemical etching of the gold donor phase, the exposed PMMA donor phase was etched away by oxygen RIE treatment for 2 min, which was performed during the formation of a ncp PS colloidal crystal. The PMMA donor phase was etched by oxygen RIE into individual disks within 1 min; the edge of the PMMA donor disk then was over etched to a smaller size until the exposed part was totally etched away (shown in Figure S2 in the Supporting Information). In order to mark the PMMA donor disk in these polymeric HPs, 4-DPAB with blue fluorescence was mixed into the PMMA phase. Figures 6A, 6B, and 6C show the SEM, optical, and fluorescence images of the free-standing binary PS-PMMA HPs, respectively. The SEM image revealed that the PS-PMMA HPs possess similar morphology as the PS-Au HPs. Most of the PS colloidal spheres were attached with PMMA donor disks, indicating that the polymeric HPs also were stable. Optical and fluorescence images show that the PS seed particles are dark, whereas the PMMA donor disks are emitting blue light, because of the 4-DPAB. The illumination of 4-DPAB is not affected by the RIE and thermal treatment. The RIE treatment used here to generate the binary polymeric HPs could manage a larger range of feature sizes from tens of nanometers to tens of micrometers, compared with the wet chemical etching described above. The size of binary polymeric HPs can thus be tuned over quite a wide range.

For the polymer−semiconductor HPs, a similar fabrication procedure was carried out, except for the etching of the exposed donor phase. Here, we took PS-Si HPs as an example. The exposed Si donor phase was etched away by RIE treatment with a gas mixture of CHF_3 at 30 sccm and SF_6 at 4 sccm. Figure 7 shows the free-standing PS-Si HPs with Si domains 200 nm thick (Figure 7A) and 40 nm thick (Figure 7B). Since the PS sphere masks are hardly reduced throughout the Si-etching

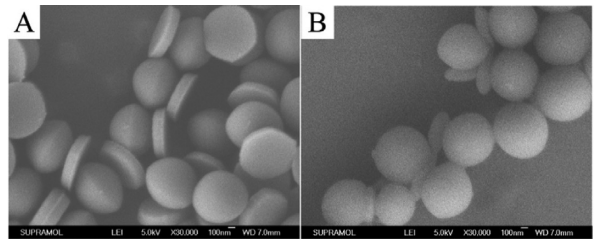

Figure 7. SEM images of the PS-Si hybrid particles with (A) thick and (B) thin Si disks. The thickness of the Si donor phase was 200 nm (panel (A)) and 40 nm (panel (B)), respectively. The diameter of the original PS seed particles was 1 μm.

process, the thickness of the Si donor phase can be tuned from several tens of nanometers to hundreds of nanometers, and the size is determined by the maximal horizontal diameter of the PS sphere mask (revealed in Scheme 1, step IV). Apparently, the thick Si film was too strong to be bent according to the sphere surface, and there it became detached as a flat disk, whereas the thin film followed the curvature and remained fixed to the sphere.

3.3. Preparation of Ternary Hybrid Particles. Based on the binary HPs fabricated above, ternary HPs could be generated by simple one-step physical vapor deposition. Utilizing controllable physical vapor deposition, metallic caps were coated on the upper hemispheres of the as-prepared binary HPs, while during the deposition process, a metal film was inevitably deposited both on the upper half of the PS spheres and the sacrificial layer. The metal film deposited on the sacrificial layer would also be removed from the substrate when releasing the ternary HPs into the dispersion and could hardly be segregated. In order to get the ternary HPs alone and leaving the metal film on the substrate, a thinner photoresist film with thickness of 30 nm was used in the preparation of ternary HPs. After the binary HPs were fabricated, the samples were treated by O_2 plasma for 5−10 min, the exposed sacrificial layer was etched away, and the original substrate was successfully exposed, which is shown in Scheme 1, step VII. Nickel was deposited afterward on the binary HPs at an incidence angle of 0° to generate the ternary HPs. When releasing the as-prepared ternary HPs from the substrate by dissolving the sacrificial layer with KOH aqueous solution (1 M) or ethanol, the metal film deposited on the substrate would not be distracted, as was revealed in Scheme 1, step IX. This procedure is shown in Figure S3 in the Supporting Information. The metal film on the substrate was intact while the majority of the ternary HPs were successfully released from the substrate.

After several times of centrifugation and sonication with water and ethanol, the ternary HPs were suspended on a Si wafer or a copper grid for SEM, EDS mapping, and TEM imaging, shown in Figure 8. The ternary HPs were also stable

Figure 6. (A) SEM, (B) optical transmission microscopy, and (C) fluorescence microscopy images of binary PS-PMMA HPs. The scale bars are 1 μm.

dx.doi.org/10.1021/cm3024692 | *Chem. Mater.* 2012, 24, 4549−4555

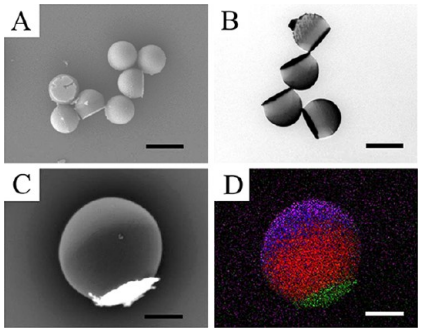

Figure 8. (A) SEM image of nickel-capped PS-Au ternary HPs and (B) TEM image of nickel-capped PS-Au ternary HPs; the nickel cap was deposited at an incidence angle of 0° for 20 nm. (C) SEM image of copper-capped PS-Au ternary HPs, and (D) the corresponding EDS mapping. The original diameter of PS seed spheres is 3.14 μm, which could get better EDS mapping. The copper cap was deposited at an incidence angle of 0° for 15 nm. The red dots in D represent carbon; green dots represent gold; and purple dots represent copper. Scale bars = 1 μm.

after mild sonication and centrifugation, and the morphology was well-maintained. In Figure 8, both the gold donor disks and the metal caps are clearly observed. Ternary HPs modified with gold donor disks and copper caps were also fabricated, and the SEM images and EDS mappings (Figures 8C and 8D) showed well-defined distribution. The silver-capped PS-Au ternary HPs were also fabricated through similar process (Figure S4 in the Supporting Information), indicating the ternary HPs could be generated by a wide range of materials, as long as they could be physically vapor deposited.

Ternary HPs combining magnetic and luminescent properties were also generated, using 4-DAPB@PMMA as polymer donor disks and nickel caps deposited on the top as the ternary part. The as-prepared ternary HPs were well-dispersed in ethanol without an external magnetic field, and showed blue luminescence under 365-nm ultraviolet light very well, as shown in Figure S5 in the Supporting Information. While under external magnetic field, the ternary HPs quickly gathered to the magnetic side within 1 min, and the luminescence of 4-DAPB was well sustained at the same time. The as-prepared ternary HPs differ in shape on the opposite poles, and both can be modified with functional patches, which may provide a brand new form of building blocks for self-assembly.

4. CONCLUSIONS

In this paper, we demonstrated a versatile approach to generate binary and ternary hybrid particles with controlled size, shape, composition, and morphology. Combining colloidal lithography (CL), thermal treatment and proper etching, polymer−metallic, polymer−semiconductor, and heterogeneous polymeric particles can be fabricated. We have extended the known processes of CL combined with plasma etching, by forming contacts between parts of a donor phase and the colloidal particle, and the strength, size, and shape of the contact can be manipulated by etching conditions, heat treatment, and layer type and thickness. Using controllable thermal treatment hybrid patches can successfully be attached onto the original seed microspheres. Based on this feature, the original seed microspheres can easily be replaced by other polymeric spheres, thus expanding the potential of the approach. This way of fabrication can be expanded in addition to any combination of materials that can be etched. Furthermore, ternary hybrid particles (HPs) can be generated by physical vapor deposition on the basis of binary HPs. The integration of functionalities of HPs may provide unique properties of magnetic, luminescent, and plasmonic devices. Above all, because of their uniform size but anisotropy in structure and composition, these binary and ternary HPs are expected to find use as a novel class of building blocks for fabricating photonic devices via self-assembly.

■ ASSOCIATED CONTENT

Supporting Information

Detailed fabricating information, expanding on that given in the Experimental Section. SEM images coupled with EDS mappings of PS-Au binary HPs and Ag-capped PS-Au ternary HPs are shown in Figures S1 and S4; optical and fluorescence microscopy images of 4-DPAB@PMMA disk arrays generated by RIE treatment using 3-μm PS sphere arrays as masks are shown in Figure S2; SEM images of nickel networks left on the substrate after the ternary HPs were released from the substrate shown in Figure S3; and optical and fluorescence photographs of nickel-capped PS-PMMA ternary HPs doping with 4-DPAB with and without external magnetic field are shown in Figure S5. This material is available free of charge via the Internet at http://pubs.acs.org.

■ AUTHOR INFORMATION

Corresponding Author

*Fax: +86 431 85193423. E-mail: gang@jlu.edu.cn.

Notes

The authors declare no competing financial interest.

■ ACKNOWLEDGMENTS

This work was supported by the National Natural Science Foundation of China (Nos. 51073070 and 51173068).

■ REFERENCES

(1) Takei, H.; Shimizu, N. *Langmuir* **1997**, *13*, 1865−1868.
(2) Love, J.; Gates, B.; Wolfe, D.; Paul, K.; Whitesides, G. *Nano Lett.* **2002**, *2*, 891−894.
(3) Correa-Duarte, M.; Salgueirino-Maceira, V.; Rodriguez-Gonzalez, B.; Liz-Marzan, L.; Kosiorek, A.; Kandulski, W.; Giersig, M. *Adv. Mater.* **2005**, *17*, 2014−2018.
(4) Pawar, A. B.; Kretzschmar, I. *Langmuir* **2009**, *25*, 9057−9063.
(5) Xia, Y.; Yin, Y.; Lu, Y.; McLellan, J. *Adv. Funct. Mater.* **2003**, *13*, 907−918.
(6) Gu, H.; Zheng, R.; Zhang, X.; Xu, B. *J. Am. Chem. Soc.* **2004**, *126*, 5664−5665.
(7) Kim, J.; Larsen, R.; Weitz, D. *J. Am. Chem. Soc.* **2006**, *128*, 14374−14377.
(8) Reculusa, S.; Poncet-Legrand, C.; Ravaine, S.; Mingotaud, C.; Duguet, E.; Bourgeat-Lami, E. *Chem. Mater.* **2002**, *14*, 2354−2359.
(9) Yu, H.; Chen, M.; Rice, P.; Wang, S.; White, R.; Sun, S. *Nano Lett.* **2005**, *5*, 379−382.
(10) Nagao, D.; Hashimoto, M.; Hayasaka, K.; Konno, M. *Macromol. Rapid Commun.* **2008**, *29*, 1484−1488.
(11) Nie, Z.; Li, W.; Seo, M.; Xu, S.; Kumacheva, E. *J. Am. Chem. Soc.* **2006**, *128*, 9408−9412.
(12) Sundararajan, S.; Lammert, P. E.; Zudans, A. W.; Crespi, V. H.; Sen, A. *Nano Lett.* **2008**, *8*, 1271−1276.
(13) Forster, J. D.; Park, J.; Mittal, M.; Noh, H.; Schreck, C. F.; O'Hern, C. S.; Cao, H.; Furst, E. M.; Dufresne, E. R. *ACS Nano* **2011**, *5*, 6695−6700.
(14) Glotzer, S. C.; Solomon, M. J. *Nat. Mater.* **2007**, *6*, 557−562.
(15) Yunker, P. J.; Gratale, M.; Lohr, M. A.; Still, T.; Lubensky, T. C.; Yodh, A. G. *Phys. Rev. Lett.* **2012**, *108*, 228303(5).

(16) Yunker, P. J.; Still, T.; Lohr, M. A.; Yodh, A. G. *Nature* **2011**, *476*, 308−311.
(17) Erb, R. M.; Jenness, N. J.; Clark, R. L.; Yellen, B. B. *Adv. Mater.* **2009**, *21*, 4825−4829.
(18) Hanarp, P.; Käll, M.; Sutherland, D. S. *J. Phys. Chem. B* **2003**, *107*, 5768−5772.
(19) Yoon, T. J.; Kim, J. S.; Kim, B. G.; Yu, K. N.; Cho, M. H.; Lee, J. K. *Angew. Chem., Int. Ed.* **2005**, *44*, 1068−1071.
(20) Chen, Q.; Diesel, E.; Whitmer, J. K.; Bae, S. C.; Luijten, E.; Granick, S. *J. Am. Chem. Soc.* **2011**, *133*, 7725−7727.
(21) Sacanna, S.; Rossi, L.; Pine, D. J. *J. Am. Chem. Soc.* **2012**, *134*, 6112−6115.
(22) Li, J. R.; Lusker, K. L.; Yu, J. J.; Garno, J. C. *ACS Nano* **2009**, *3*, 2023−2035.
(23) Li, X.; Wang, T. Q.; Zhang, J. H.; Zhu, D. F.; Zhang, X.; Ning, Y.; Zhang, H.; Yang, B. *ACS Nano* **2010**, *4*, 4350−4360.
(24) Kosiorek, A.; Kandulski, W.; Glaczynska, H.; Giersig, M. *Small* **2005**, *1*, 439−444.
(25) Zhang, G.; Wang, D. Y.; Möhwald, H. *Nano Lett.* **2007**, *7*, 127−132.
(26) Zhou, X. D.; Knoll, W.; Zhang, N.; Liu, H. *J. Nanopart. Res.* **2009**, *11*, 1065−1074.
(27) Ye, J.; Dorpe, P. V.; Roy, W. V.; Borghs, G.; Maes, G. *Langmuir* **2009**, *25*, 1822−1827.
(28) Li, C.; Hong, G. S.; Qi, L. M. *Chem. Mater.* **2010**, *22*, 476−481.
(29) Xu, M. J.; Lu, N.; Xu, H. B.; Qi, D. P.; Wang, Y. D.; Chi, L. F. *Langmuir* **2009**, *25*, 11216−11220.
(30) Ye, S.; Carroll, R. L. *ACS Appl. Mater. Interfaces* **2010**, *2*, 616−620.
(31) Zhang, G.; Wang, D. Y.; Möhwald, H. *Chem. Mater.* **2006**, *18*, 3985−3992.
(32) Lu, Y.; Xiong, H.; Jiang, X. C.; Xia, Y. N. *J. Am. Chem. Soc.* **2003**, *125*, 12724−12725.
(33) Zhang, J. H.; Chen, Z.; Wang, Z. L.; Zhang, W. Y.; Ming, N. B. *Mater. Lett.* **2003**, *57*, 4466−4470.
(34) Rybczynski, J.; Ebels, U.; Giesig, M. *Colloids Surf. A* **2003**, *219*, 1−6.